
Functional magnetic resonance imaging: imaging techniques and contrast mechanisms

Alistair M. Howseman^{1†} and Richard W. Bowtell²

¹Wellcome Department of Cognitive Neurology, Institute of Neurology, Queen Square, London WC1N 3BG, UK

²Magnetic Resonance Centre, School of Physics and Astronomy, University of Nottingham, Nottingham NG7 2RD, UK

Functional magnetic resonance imaging (fMRI) is a widely used technique for generating images or maps of human brain activity. The applications of the technique are widespread in cognitive neuroscience and it is hoped they will eventually extend into clinical practice. The activation signal measured with fMRI is predicated on indirectly measuring changes in the concentration of deoxyhaemoglobin which arise from an increase in blood oxygenation in the vicinity of neuronal firing. The exact mechanisms of this blood oxygenation level dependent (BOLD) contrast are highly complex. The signal measured is dependent on both the underlying physiological events and the imaging physics. BOLD contrast, although sensitive, is not a quantifiable measure of neuronal activity. A number of different imaging techniques and parameters can be used for fMRI, the choice of which depends on the particular requirements of each functional imaging experiment. The high-speed MRI technique, echo-planar imaging provides the basis for most fMRI experiments. The problems inherent to this method and the ways in which these may be overcome are particularly important in the move towards performing functional studies on higher field MRI systems. Future developments in techniques and hardware are also likely to enhance the measurement of brain activity using MRI.

Keywords: fMRI; echo-planar imaging; BOLD contrast; brain mapping

1. INTRODUCTION

Functional neuroimaging using nuclear magnetic resonance (NMR) is approaching the end of its first decade as a scientific discipline. During that time the technique has evolved with great speed from being a potentially useful tool into arguably the most powerful method available for generating maps of neuronal activity in the human brain. This development has seen the technique move from the domain of the magnetic resonance imaging (MRI) research laboratory into the arena of dedicated centres for functional neuroimaging populated by neuroscientists, psychologists and psychiatrists with, in some cases, few MRI specialists. A large body of research has already been generated using functional MRI (fMRI) to study brain function in healthy volunteers. Among others, the following fields have been investigated: vision (Tootell *et al.* 1998), motor (Ashe & Ugurbil 1994), language (Binder 1997), memory (Fletcher *et al.* 1997), emotion (Phillips *et al.* 1997; Schneider *et al.* 1997) and pain (Davis *et al.* 1997). Many studies have also been performed in patient populations, although these entail additional and varied difficulties. The technique has been used in the fields of stroke (Leifer *et al.* 1998; Thulborn *et al.* 1998), amputation and phantom limbs (Lotze *et al.* 1998), presurgical planning (Bittar *et al.* 1998; Lehericy *et al.* 1998; McCarthy 1998), epilepsy (Jackson *et al.* 1994; Graveline *et al.* 1998) and various

psychiatric disorders (see Fu & McGuire, this issue). The extent to which the theoretical, statistical (see Petersson *et al.*, both papers in this issue) and practical difficulties associated with these studies can be overcome will define the clinical value of fMRI and this in turn will ultimately determine the number of MRI systems installed with functional imaging capability.

The remarkable speed with which the fMRI technique has become a valuable tool in imaging neuroscience is largely due to the fact that several of the core ingredients which make up fMRI methodology were already at an advanced level of development when the potential to image brain function using MRI first became apparent. In particular, by the early 1990s the established field of functional imaging using positron emission tomography (PET) (Lassen *et al.* 1991) had seen the development of ideas about (i) the design of experiments to generate images of cognitive processing, and (ii) methods of processing data to yield statistical images reflecting brain activity associated with those cognitive functions (for overview, see Frackowiak *et al.* 1997). The acquisition of functional imaging data using a non-invasive method (MRI) with spatial and temporal resolution superior to that of PET was rapidly embraced by this research community. The rapid growth of fMRI has also been facilitated by recent developments in NMR imaging methods and instrumentation. MRI has been in widespread clinical use since the early 1980s and MRI manufacturers now provide highly optimized MRI systems. Two technical factors have been especially important in the development of fMRI. First, the speed of

[†]Present address: SMIS Ltd, 10 Alan Turing Road, Surrey Research Park, Guildford, Surrey GU2 5YF, UK.

the imaging method needs to be such that data from the entire brain can be acquired in a time less than the duration of the brain states induced by the presentation of stimuli. This requirement is fulfilled by echo-planar imaging (EPI), which was initially proposed in the earliest days of MRI (Mansfield 1977), but which was not available on clinical MRI systems until recently because of the technical difficulties associated with EPI (for overview of EPI, see Schmitt *et al.* (1998)). The second aspect of scanner technology which has been especially important in allowing sophisticated fMRI studies to be performed is the ever-increasing computing power available, which facilitates the acquisition, processing and storage of very large data sets.

Although the first fMRI experiments (Belliveau *et al.* 1991) used an exogenous gadolinium-based contrast agent this technique was rapidly superseded by the discovery that deoxyhaemoglobin could be used as an endogenous contrast agent (Ogawa *et al.* 1990). This so-called blood oxygenation level dependent (BOLD) contrast has proved to be a very sensitive MRI marker of neuronal activity at magnetic field strengths of 1.5 T and above. The sensitivity of BOLD contrast is such that experiments can be performed in individual subjects, with temporal resolution on the scale of hundreds of milliseconds to seconds and spatial resolution of 3 mm or less, in almost all cortical and subcortical structures in the brain.

This article will briefly describe the mechanisms which generate contrast in fMRI and will discuss the different imaging techniques which are employed. There remain outstanding issues regarding the level of accuracy with which BOLD contrast reflects neuronal activity. Furthermore BOLD contrast remains essentially non-quantifiable. These and other problems associated with the fMRI technique will be addressed, including the image artefacts which pose an ever greater problem at higher magnetic field strength.

2. BOLD CONTRAST IN MRI

(a) *Principles of MRI and BOLD contrast*

NMR image intensity reflects the concentration of water within a sample and is also dependent on the chemical and physical environment in which the water molecules reside (for review, see Gadian 1995). Image contrast in MRI can be varied through the choice of imaging parameters, and in fMRI contrast is tailored to optimize the signal dependence on deoxyhaemoglobin concentration ([rHb]). The MRI signal arises from the stimulation of transitions between the nuclear spin energy levels of the hydrogen atoms in water, placed in a large magnetic field. These transitions are induced by the application of radio-frequency (RF) energy at a specific (resonance) frequency which is proportional to the strength of the magnetic field. An NMR signal is detected, at the resonance frequency, as a voltage across a tuned RF coil. Images of the distribution of water are created using magnetic field gradients which impose a linear relationship between the NMR frequency and spatial location. NMR relaxation is the process by which the perturbed nuclear spin system returns to thermal equilibrium after the application of a pulse of RF energy. A relaxation property which is dependent on the range of

NMR frequencies within an image voxel, and is described by a time constant T_2^* , is the source of BOLD contrast. T_2^* is affected by random processes involving interactions between nuclear spins as well as by magnetic field inhomogeneity, which can result from either macroscopic magnetic susceptibility differences in the head or the microscopic effects of paramagnetic substances. While biological samples are primarily diamagnetic, deoxyhaemoglobin is paramagnetic and its concentration affects the value of T_2^* in a voxel due to the microscopic magnetic field gradients established in its vicinity. This mechanism can give rise to BOLD contrast on MR images which are sensitive to magnetic field inhomogeneity, that is, T_2^* -weighted images (Ogawa *et al.* 1990). By using EPI it is possible to image changes in blood oxygenation levels very rapidly (Turner *et al.* 1991).

A robust way to generate BOLD contrast is to continually acquire MR images while subjects are presented with blocks of sensory stimulation, of duration approximately 30 s, interspersed with intervals of rest (Ogawa *et al.* 1992; Kwong *et al.* 1992; Bandettini *et al.* 1992). Simply, the average baseline (resting) condition image is subtracted from the image corresponding to the average of the stimulation condition. The difference images show BOLD contrast in regions where the stimulated neuronal activity leads to a reduction in [rHb]. This occurs because a localized increase in regional cerebral blood flow (rCBF) associated with neuronal firing is accompanied by a relatively smaller increase in the use of oxygen, an effect first described by PET studies using ^{15}O labelling (Fox & Raichle 1986; Fox *et al.* 1988). The reduction in [rHb] leads to smaller local field gradients, which results in less signal loss due to spin dephasing (i.e. an increase in T_2^*) and a consequent increase in the level of the MRI signal (Ogawa *et al.* 1990, 1992).

The magnitude of the signal change which can be generated by BOLD contrast has been the subject of vigorous debate since the earliest reports of fMRI. In several early fMRI studies which made use of fast gradient echo imaging techniques a component of T_1 contrast was inadvertently included in the functional signal change and this could lead to large (tens of per cent) changes (Frahm *et al.* 1993). However, it quickly became apparent (Kim *et al.* 1994; Frahm *et al.* 1994) that these signals, which are due to blood in large vessels flowing into the imaging slice, are less well localized to neuronal activity than the BOLD signal. Most fMRI experiments performed today use sequences which ensure that the T_1 component is minimal (Howseman *et al.* 1999). Despite the clarification that T_1 contrast should be avoided, the debate regarding signal magnitude continues. There are so many factors affecting the measured signal changes (how a region of interest is selected, field strength, several imaging parameters etc.) that comparisons between studies are difficult. However, this issue is important because it is related to which part of the vasculature yields the dominant signal change and therefore how accurately the spatial distribution of fMRI signals reflects neuronal activity. In general, BOLD contrast represents a qualitative rather than a quantitative measure of brain activity because the relationship between the signal change in T_2^* -weighted images and

the underlying vascular geometry and distribution of deoxyhaemoglobin is not easily modelled. Essentially the problem is that many image voxels contain very heterogeneous distributions of vessels. The voxel size in a typical fMRI data set is of the order of $3\text{ mm} \times 3\text{ mm} \times 3\text{ mm}$ ($27\text{ }\mu\text{l}$). At this scale any voxel may contain blood vessels ranging from capillaries ($5\text{ }\mu\text{m}$ diameter) and venules ($10\text{--}30\text{ }\mu\text{m}$) up to pial veins ($100\text{--}400\text{ }\mu\text{m}$) and larger draining veins. Only vessels on the venous side of the circulation are subject to oxygenation changes and only those close enough to the site of neuronal activity will contribute to BOLD contrast. Further downstream the effects are gradually diluted. The signal change measured in a voxel will therefore reflect how the underlying physiological events alter the distribution of [rHb] and how the geometry of the vessels impact on the physics of the BOLD contrast mechanism.

If contributions to BOLD contrast were limited to intravascular signals then the small fractional blood volume in the brain would severely limit the MRI signal changes due to [rHb] changes. However, because the mechanism by which BOLD occurs involves the magnetic field gradients which surround deoxyhaemoglobin, these gradients can extend into the surrounding tissue and so a higher proportion of water can be affected (Ogawa *et al.* 1990). This effect has been analysed with a Monte Carlo simulation of a biophysical model which assumes a homogeneous distribution of vessels (Ogawa *et al.* 1993). The model indicates that, with 75% of the blood volume in a voxel found in capillaries and 25% in venules, the BOLD signal change in a T_2^* image acquired at an optimal echo time (TE) at 4 T would be approximately 8%. Additionally the model predicts that at higher field strength the (extravascular) capillary component of BOLD contrast becomes relatively more significant than that from venules and pial veins. At a lower field strength of 1.5 T it has been suggested that the intravascular water is the dominant source of the BOLD signal (Boxerman *et al.* 1995), a theory which is supported by experimental evidence that when large spoiler (diffusion) gradients are applied most of the BOLD signal is removed as the intravascular component is dephased. However, in a series of experiments in rats at 2.0 T and humans at 1.5 T using intravascular contrast agents, Zhong *et al.* (1998) argue that there is also a significant extravascular component of BOLD contrast at these field strengths. Although the theoretical predictions are that BOLD contrast should be less than a few per cent at field strengths up to 2 T, there is much experimental evidence of larger changes in T_2^* -weighted images (Lai *et al.* 1993; Frahm *et al.* 1994; Howseman *et al.* 1999). It has been proposed that these larger percentage changes may occur, if a significant fraction of a voxel is filled by a large vessel, as a result of simple bulk phase changes occurring in the vessel during activation (Haacke *et al.* 1994).

There are techniques, including the use of diffusion gradients, which allow partial discrimination between BOLD signals which arise purely from the capillary bed and those which occur in larger vessels (Boxerman *et al.* 1995; Lee *et al.* 1995; Song *et al.* 1996). Although it is desirable that fMRI contrast should reflect activity in grey matter it is probably unrealistic to expect that good sensitivity can be maintained at a field strength of 1.5 T if

all the signal from the larger vessels is removed. Nearly all fMRI experiments are performed using T_2^* -based imaging. However, it is also possible to generate contrast using T_2 -weighted imaging with a spin echo sequence. In T_2 imaging the dephasing which leads to signal decay is due only to random processes and not to dephasing due to static inhomogeneities. [rHb] can affect T_2 because of the diffusion of water molecules through the microscopic field gradients. The contrast due to functional activation on T_2 images is much smaller than on T_2^* images, hence its limited use, although simulations suggest (Ogawa *et al.* 1993; Weisskoff *et al.* 1994) that this is partly because large vessels contribute much less to the signal. Bandettini *et al.* (1994b) estimate that the ratio between the contrast generated by gradient echo and spin echo fMRI in the same region is about 2, when both techniques are optimized.

(b) Relationship between BOLD and physiology

A comprehensive review of how the relationship between neuronal activity, rCBF and metabolic activity affects PET data is given by Jueptner & Weiller (1995). With PET the key issue is how well rCBF changes correlate with neuronal activity. In fMRI the relationship between image contrast and neuronal activity is dependent on a complex set of factors which determine the spatio-temporal changes in [rHb]. An increase in blood flow and an increase in blood volume accompany the onset of neuronal firing. The balance between these processes and the rate at which oxygen is metabolized ([rCMRO₂]) determine the local [rHb] although the correlation between [rHb] and neuronal firing may be nonlinear and temporally varying. Evidence about the relationship between blood flow increases and the use of oxygen has been provided by direct optical measurements in the exposed visual cortex of cat brain (Malonek & Grinvald 1996). These experiments show that the response to sensory stimulation is an initial phase (*ca.* 3 s) of hypo-oxygenation which is highly localized to individual cortical columns followed by an extended phase (several seconds) of hyperoxygenation which is more widely dispersed (up to 5 mm). Broadly, the temporal characteristic of this response is in accord with that measured by fMRI, although the optical data suggest that a rather larger initial dip in the BOLD response would be expected than that which has been measured (Menon *et al.* 1995). Crucially, the optical data raise the possibility that the main (positive) part of the BOLD response is not so well localized and therefore the true functional resolution of fMRI may be limited not by the imaging resolution itself but by the spatial extent of the physiological changes arising within the vicinity of neuronal firing. More restricted functional localization by using the initial dip has been verified with fMRI at high field in human visual cortex (Hu *et al.* 1997) and simulations support the hypothesis that there can be a localized T_2^* effect due to increased oxygen extraction prior to changes in rCBF and blood volume (Dymond & Norris 1997). However, before designating the delayed positive part of the BOLD response as being too widespread to provide high-resolution localization, it is salutary to consider the study of Yang *et al.* (1997b) in which they show that positive BOLD contrast has the same spatial

pattern and extent as the measured electrical activity in individual rat whisker barrels.

The temporal characteristics of the BOLD response are important not only because they relate to the physiological events underpinning BOLD contrast but because they also impact on experimental design and data processing. The form of the haemodynamic response function (HRF) measured in fMRI can vary in timing from brain region to region, but is broadly similar. An initial very small signal decrease of about 1 s duration, which is more easily measured at high field (Menon *et al.* 1995; Hu *et al.* 1997), is followed by the BOLD signal increase which peaks between 4 and 8 s after the onset of stimulation (Friston *et al.* 1994). After the end of stimulation the signal exhibits a small undershoot which returns to baseline over tens of seconds (Janz *et al.* 1997; Fransson *et al.* 1998). A report that during extended stimulation the BOLD signal decays to baseline due to a recoupling of flow and metabolism (Frahm *et al.* 1996; Kruger *et al.* 1996) has not been confirmed to be a general phenomenon in other studies (Bandettini *et al.* 1997; Howseman *et al.* 1998). Consequently it is currently widely accepted that the HRF can be convolved with the experimental design as a model for expected activity during fMRI analysis; that is, the haemodynamic response which leads to BOLD is time invariant during the duration of an experiment. However, it has also been shown that there may be nonlinear components in the magnitude of the response if the rate at which distinct individual stimuli are presented is high (Friston *et al.* 1998a). This analysis is based on experimental data from a direct comparison between PET and fMRI (Rees *et al.* 1997), which showed that as the rate at which words were presented to a subject increased, a measured linear increase in rCBF was not mirrored by a linear increase in the amplitude of BOLD, the BOLD response starting to saturate with word rates above 30 per minute. These data strongly suggest that the extraction of oxygen increases nonlinearly as the neuronal activity increases because the linear increase in rCBF is expected to correlate well with the neuronal firing rate (Jueptner & Weiller 1995). This finding has clear implications for theoretical models of the coupling between rCBF and oxygen metabolism and especially needs to be considered in event-related fMRI studies (Rosen *et al.* 1998; Josephs & Henson, this issue). In figure 1 the excellent correspondence between the activation images produced using PET and fMRI in the Rees *et al.* (1997) study is shown.

A recent model incorporating the effects of dynamic changes in blood oxygenation and blood volume provides an explanation for the form of the BOLD HRF (Buxton & Frank 1997; Buxton *et al.* 1998). This model is based on the premise that there is a strong coupling between blood flow and oxygen metabolism but that the biophysics of oxygen extraction determines that a large increase in flow is required to support a small increase in oxygen metabolism. This so-called balloon model, which assumes that the capillary volume remains fixed, but allows for an expandable volume in the venous part of the vascular bed, can predict the transient aspects of the BOLD response. Perhaps one of the most important aspects of such work in future will be an integrated model of the spatial and temporal behaviour of BOLD because recent

studies have further highlighted the spatio-temporal complexity of the BOLD response. Using sustained visual stimulation, Chen *et al.* (1998) found that there was evidence for transient responses as seen by Frahm *et al.* (1996) in large vessels, but a sustained response in cortical grey matter. Also, measurement of the delay between the onset of haemodynamic change and when maximum signal change occurs has shown that the capillary-based signal reaches a maximum several seconds before that from larger vessels (Lee *et al.* 1995).

The broad BOLD HRF imposes a limit to the temporal resolution of fMRI in detecting individual brain events, although the ultimate resolution which may be obtained with good experimental design may be rather better than may be expected from an HRF of several seconds lag and width. In the same brain region the detectability of discrete responses is no better than 3–5 s (Bandettini 1993; Kim *et al.* 1997). However, differences in the onset of activity in different regions are detectable to approximately an order of magnitude better than this if some signal averaging is used (DeYoe *et al.* 1992; Hykin *et al.* 1995; Savoy *et al.* 1995). The measurement of differences between regions should be treated with some caution, however, because they are likely to reflect different latencies in the HRF as well as differences in the timing of neuronal activity. It has been shown that BOLD contrast can be generated by stimuli as short as a few tens of milliseconds (Savoy *et al.* 1995). The differences between responses to different sorts of single events can be measured to an accuracy much greater than the HRF width. By comparing the responses to words which were either novel or had previously been seen, Friston *et al.* (1998b) have shown that fMRI can discriminate between dynamics in a single region on a 100 ms time-scale.

In experiments which aim to image functional segregation of relatively large cortical areas, the current limited understanding of the degree to which BOLD contrast accurately reflects the spatial extent of neuronal activity is perhaps unimportant. The BOLD technique yields signal changes located at least within 10 mm of the site of neuronal firing, which is quite adequate in many cases. However, in experiments in which higher functional resolution is required then difficulties may be encountered in generating contrast with sufficient resolution. An example of this is a study which attempted to image the functional differences between the stripe and interstripe activity in area V2 in human visual cortex but found that T_2^* contrast was not sufficiently specific to yield functional differences (Thulborn *et al.* 1997). In this same study there is evidence that, by using T_2 contrast to be preferentially sensitive to the microvasculature, higher functional resolution in the fMRI data can be obtained. This interesting prospect will warrant extended study as more investigations are performed on high-field systems.

3. fMRI TECHNIQUES

Several high-speed imaging methods have been used for fMRI, most of which are based on the principles of EPI. Although to some extent the diversity of techniques currently being used at different sites reflects the sequences

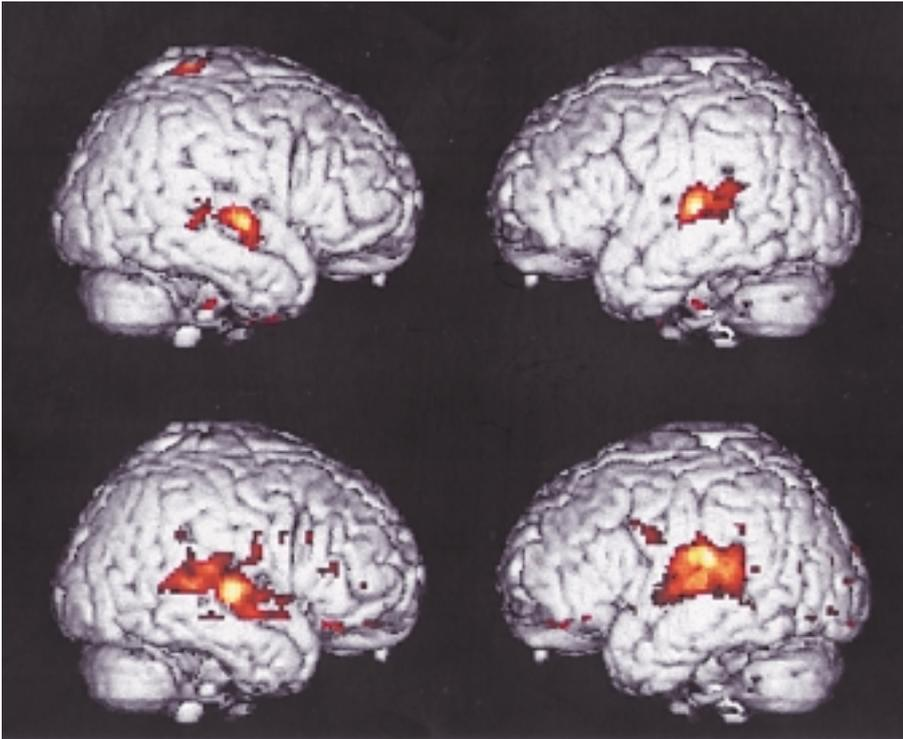


Figure 1. fMRI activation images acquired at 2 T (bottom) and PET activation images (top) from the same male subject in a comparative study between the two modalities. The activation in auditory cortex is due to a parametric analysis of the subject listening to words at different rates of presentation. The sound of the MR scanner was recorded and played to the subject during the PET study to simulate the potential confound in the MRI data.

provided by the different system manufacturers, a range of imaging options is desirable and there is no single optimal imaging method for all fMRI experiments. Although relatively high speed is a requirement for fMRI, this leads to several trade-offs which have to be made and ultimately some temporal resolution may be sacrificed to improve other aspects of image quality. The major technical difficulty in the generation of EPI images is the switching of very large currents through the system's gradient coils.

The imaging technique that is most commonly used is multislice EPI (for a comprehensive review of EPI, see Schmitt *et al.* (1998)). Figure 2 schematically shows how image volume data are acquired in an epoch-based fMRI experiment using multislice EPI. Each image is acquired by first selectively exciting an NMR signal from a thin slice of the head, using a shaped RF pulse and a slice selection field gradient, and subsequently sampling the evolution of this signal in the presence of a rapidly switched magnetic field gradient. The switched gradient waveform generates a series of echoes of the NMR signal, which are progressively phase encoded by the action of a second orthogonal field gradient, applied as a series of 'blips' occurring at the zero crossings of the switched gradient. The set of echoes formed in this manner contains all the information necessary to construct a two-dimensional image of the slice. The image matrix size is set by the product of the number of echoes acquired and the number of data points sampled in each echo, typical values being 64×64 for fMRI experiments. Using the k -space formalism, in which the imaging sequence is viewed in terms of the measurement of a range of spatial frequencies (k) describing the object structure, the sequential acquisition of these echoes corresponds to a raster-like scan through k -space. Data at the centre of k -space, whose magnitude largely defines the image contrast, are acquired at a TE whose minimum value is set by the time needed to generate half the total number

of echoes. The sequence of the form shown in figure 2 is known as gradient echo EPI, as there is no refocusing of the dephasing effects of magnetic field homogeneities. Gradient echo EPI images thus naturally show the T_2^* weighting which is most sensitive to the level of blood oxygenation. Examples of images acquired using this method are shown in figure 3. The images have a 256×128 matrix size and are of higher resolution than usually achieved with EPI (data courtesy of Dr Steve Roberts, SMIS Ltd, Guildford, UK). These very high quality EPI images have been acquired using a head gradient and RF coil insert in a 1.5 T magnet. Using a smaller diameter gradient coil means that higher gradient strengths and faster switching times can be achieved. The total acquisition time for each image in figure 3 is 130 ms.

Volume data are built up by repeating the process of image acquisition at different slice positions. The total volume acquisition time is given by the product of the number of slices and the time between slice acquisitions. Whole-brain coverage can be achieved in approximately 5 s. Repetition of this process allows the acquisition of a number of data volumes during the different states of a functional paradigm as shown in figure 2. The time between repeated acquisition of the same slice (TR) controls the effect of T_1 relaxation on the image intensity, with short TR values giving reduced signal, and greater likelihood of the manifestation of T_1 -related in-flow effects.

Many early fMRI studies were performed using fast gradient echo, Fourier imaging methods such as FLASH (Haase *et al.* 1986) because EPI was not so widely available as it is today. These techniques can still find application because higher resolution images can be generated than with EPI, but this is at a cost of an increased time for the acquisition of each image. With these techniques, rather than scanning all k -space after a

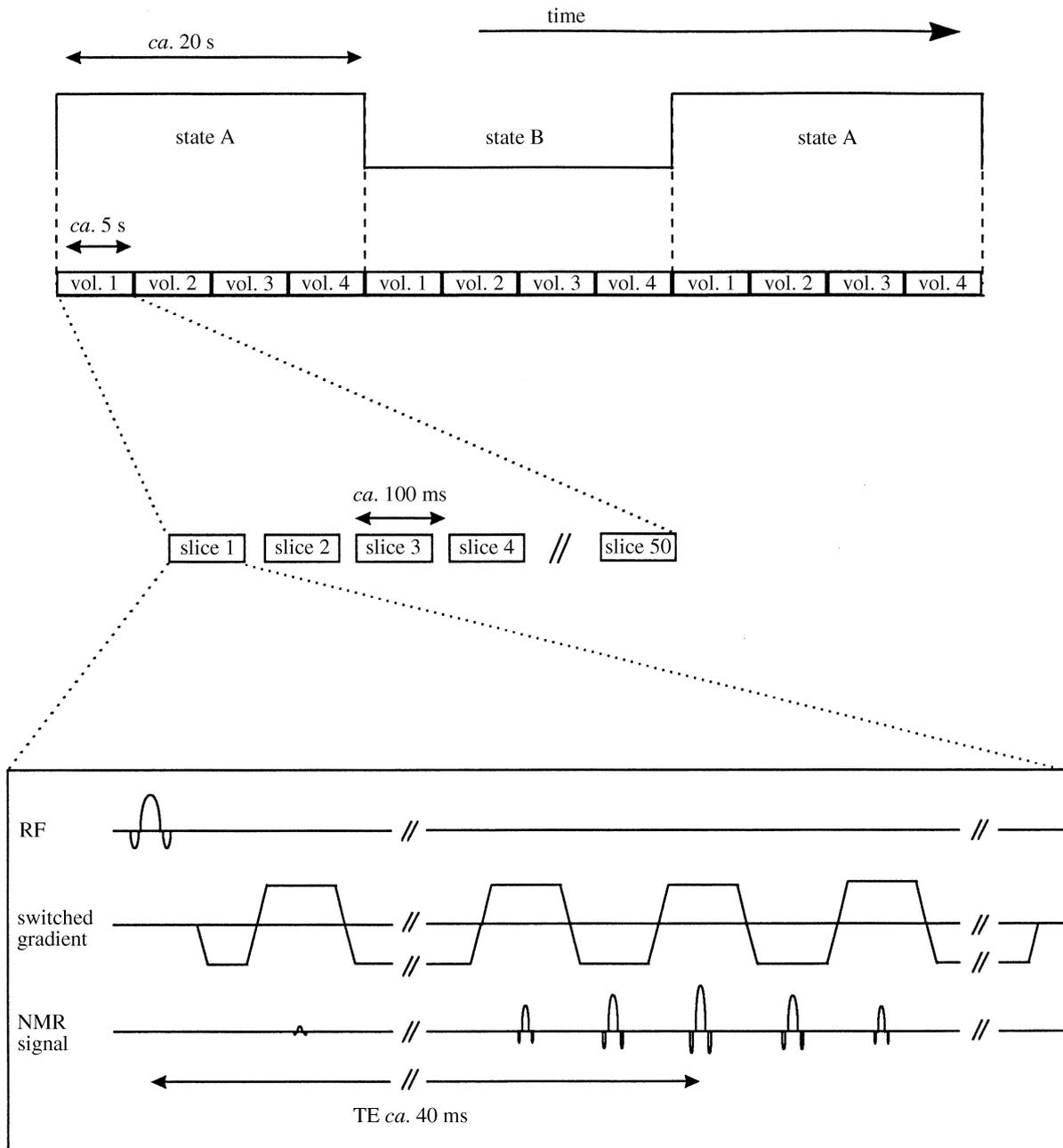


Figure 2. Schematic timing diagram of a typical state-related fMRI experiment. Data are acquired continually as two stimulus states A and B of not less than 20 s are alternated. In the example shown, during each state the entire brain is imaged four times with a multislice EPI acquisition of 50 slices. Each slice takes approximately 100 ms to acquire and the entire brain is imaged in 5 s. The order in which the slices are acquired can be selected and the effective repetition time, TR, for each slice is 5 s. The imaging method shown in the pulse sequence timing diagram is gradient echo T_2^* -weighted EPI with a TE of 40 ms.

single RF excitation, multiple excitations are used, with the data required for image reconstruction being acquired line by line. The elevated acquisition times of these techniques lead to a reduction in the temporal resolution with which the time-course of the haemodynamically mediated signal change can be monitored and therefore they are not compatible with the 'event-related' fMRI experiments (Josephs *et al.* 1998a) that are currently coming into wider use.

Very high resolution structural MRI scans with good grey-white matter contrast are usually acquired as part of an fMRI study so that the EPI data can be overlaid

onto images showing cortical structure. These high-resolution images are also usually normalized into a standard brain space (Friston *et al.* 1995) so that Talairach coordinates can be reported for functional activations. For studies involving cortical areas which are close to large draining vessels it is sometimes also useful to acquire MR venograms, which are images consisting only of slow flow in blood vessels (Haacke *et al.* 1994). Where very high functional resolution is required, such as in somatosensory cortex, an accurate delineation of the local vasculature can prove useful when determining the precise location of functional signal change.

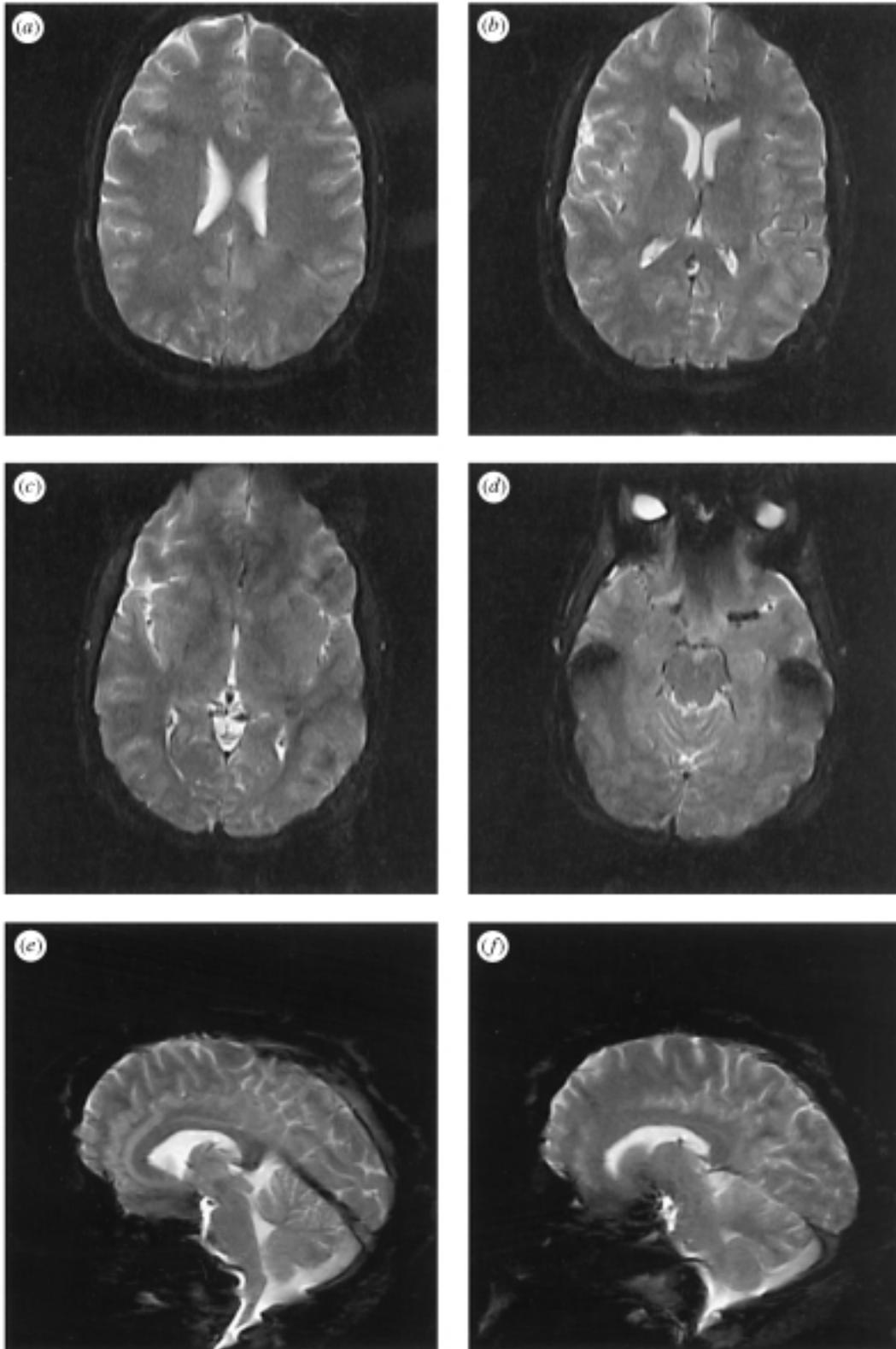


Figure 3. Single-shot gradient echo EPI images. Matrix size 256×128 , field of view 220 mm, slice thickness 4 mm, TE, 60ms. Images were acquired using a head gradient insert coil on a 1.5 T system. Data provided courtesy of Dr Steve Roberts, SMIS Ltd, Guildford, UK.

(a) *Artefacts in fMRI images*

A particular disadvantage of using any T_2^* imaging method, sensitive to microscopic field inhomogeneities to generate image contrast, is that the technique will also be sensitive to macroscopic field inhomogeneities such as those found at tissue, air and bone interfaces. The

difference in the magnetic susceptibility of these substances leads to localized magnetic field gradients being established which are inherent to the anatomical structure of the head. In the human brain these gradients are largest in the frontal pole above the air-filled sinuses, in the inferior temporal lobes where there are complex

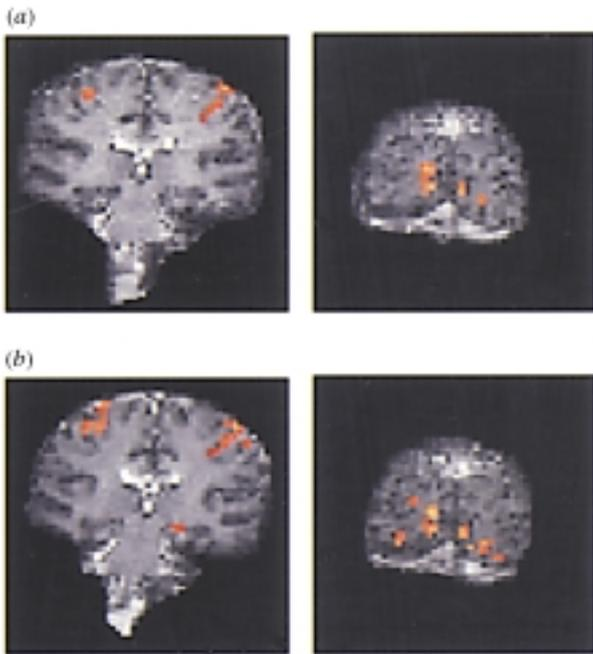


Figure 4. Two slices from an inversion recovery (1200 ms) data set acquired in the coronal orientation at 3 T. (a) Two-shot interleaved EPI acquisition. (b) Single-shot EPI acquisition. In both cases voxel dimensions are $3\text{ mm} \times 3\text{ mm} \times 3\text{ mm}$, matrix size 64×64 and gradient switching frequency 1.9 kHz. The activation shown resulted from finger tapping which was visually cued using a checker-board pattern reversing at 4 Hz. It is clear from these two slices showing motor and visual cortex, that the distortion in the two-shot images (a), which have an effective frequency per point of 60 Hz, is less than that in the single-shot images (b) which have a 30 Hz point separation in the (medio-lateral) phase encode direction.

boundaries between tissue, the petrous bone and the air passages of the ear and at the level of the cerebellum and brain stem. The consequences of these localized field gradients, which operate over several voxels in the images, are a loss of MR signal due to spin dephasing across the width of a voxel and a relocation of signal due to the additional magnetic field gradient, i.e. image distortion. An example of geometric distortion can be seen in the frontal lobe in figure 3c. The loss of signal on T_2^* -weighted images is directly related to the TE. This effect can be seen in the anterior part of the temporal lobe in figure 3d where the TE is 60 ms. By shortening the TE this signal loss can be minimized, but at the cost of a reduction in the sensitivity to BOLD contrast. By using spin echo images this signal loss can be eliminated, although, as discussed earlier, the resultant T_2 contrast is less sensitive to brain activity. A compromise between these conflicting requirements is to use a technique known as asymmetric spin echo EPI in which T_2^* contrast with a shorter effective TE can be achieved (Stables *et al.* 1998).

The geometric distortion in EPI images is very severe because of the long read-out time after each RF pulse. The problem is insignificant with techniques such as FLASH because each read-out time is short. The form of the distortion is strongly dependent on the orientation in which the images are acquired. In figure 4 severe distortion in the brain stem is seen in coronal EPI images

acquired at 3 T. Geometric distortion affects spin echo EPI in a similar way as in gradient echo EPI. Shorter EPI acquisition times reduce the distortion, but these are limited by the gradient specifications of the system. Post-processing methods to reduce geometric distortion using pre-acquired field inhomogeneity maps have been proposed (Bowtell *et al.* 1994a; Jezzard & Balaban 1995; Reber *et al.* 1998) although these have yet to find widespread use, perhaps because the severity of this problem in fMRI is still not widely recognized. However, as the demands for ever more precise localization of activity increase, then the removal of geometric distortion from the EPI data when co-registering onto the structural images will become very important.

Another artefact which is characteristic of EPI data is a low intensity ghost image which appears halfway across the image field of view. The source of this so-called Nyquist ghost is that during EPI processing the odd and even echoes need to be time reversed with respect to each other because of the polarity reversal of the imaging gradient. This time reversal introduces artefacts due to imperfections in the timing of the experiment, the generation of eddy currents, nonlinearities in the receiver filters and field inhomogeneity (Schmitt *et al.* 1998). Removal of the Nyquist ghost during post-processing reduces its level to typically around 5%. An additional complication is that the ghost level may change during the acquisition of a time-series of images and it has been shown that with the confound of stimulus correlated motion (see §4) false activation due to correlated fluctuations in the Nyquist ghost can occur (Grootoink *et al.* 1998).

(b) *Choice of imaging parameters in experimental design*

Among the important considerations when selecting an imaging method for fMRI are speed, spatial resolution, signal-to-noise ratio (SNR), level of BOLD contrast and minimization of false activation artefacts. Additionally the design of the experiment in terms of its temporal characteristics (both timing of stimuli and overall duration) and the extent of brain coverage required, may affect the choice of imaging method. If whole-brain coverage is required then some form of EPI method is essential, the only appropriate use of (low flip angle) FLASH methods being where a high-resolution study of a known activation focus is required. For fMRI using T_2^* contrast the TE should be set to approximately the value of the T_2^* of grey matter to maximize BOLD contrast, although the statistical significance of activation is a broad function of TE (Yang *et al.* 1998b). The slice thickness in multislice studies is another important parameter. The signal loss due to susceptibility gradients described above is reduced if thinner slices are acquired. However, very thin slices ($< 1\text{ mm}$) have low SNR and the number of slices needed to cover the entire brain becomes excessive. In a recent study (Howseman *et al.* 1999), it has been shown that in an area of the brain where there are no susceptibility artefacts, using broader slices (5–8 mm) provides optimal sensitivity per unit time. In the same study there is also evidence that using small gaps between slices makes the technique less sensitive to the effects of T_1 saturation when there is subject motion. Again in the

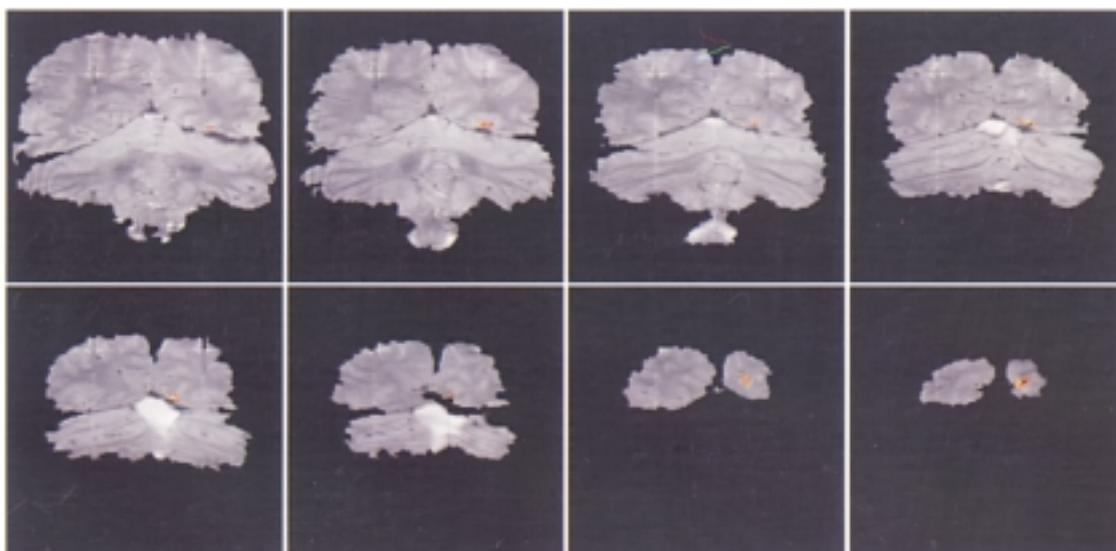


Figure 5. Very high resolution EPI images acquired using a two-shot interleaved sequence at 3 T. In-plane resolution is $0.8 \text{ mm} \times 0.9 \text{ mm}$ and slice thickness is 4.5 mm , 256×256 matrix size, gradient switching frequency 1.04 kHz . The activation shown is due to reversal at 4 Hz of a checkerboard pattern, which was presented in a small area of the right visual field only.

same study, the order in which the slices are acquired has been shown not to affect the data and so the most important aspect of slice order is how the timing of stimuli should be presented so as to avoid differential sensitivity in different parts of the brain based on the timing of the experiment alone (Price *et al.* 1999).

(c) Variants on the EPI technique

As described above the most widely used fMRI method at present is multislice EPI with either contiguous or interleaved slice acquisition. There are, however, several variants on EPI which have been used for fMRI and can potentially offer advantages of some form.

(i) Segmented EPI

One of the biggest limitations in EPI is (by MRI standards) the relatively low spatial resolution. For fMRI performed on systems using a body gradient coil, typical EPI matrix sizes are 64×64 with a resolution of 3 mm . Image matrices of 128×128 can be generated, with voxel sizes of 1.5 mm , but these require a long sampling time and lead to a higher degree of distortion. An alternative approach to improving the spatial resolution is to use two or more RF pulses and acquire a subset of the total number of required k -space lines after each. Typically the k -space lines would be interleaved because this minimizes artefacts when the sets of lines are conjoined and Fourier transformed to generate the final image. In figure 4 a reduction in geometric distortion when using segmented EPI compared with single-shot EPI can be seen. Two-shot segmented EPI has also been used to generate very high resolution 256×256 matrix images at 3 T where the read-out time needs to be kept short (Clare *et al.* 1996). Images from this study are shown in figure 5, in which very localized functional activation is seen with a visual stimulus presented in a small fraction of the right visual field. It should also be noted that the principle of k -space segmentation can be applied to any of the other techniques discussed below.

(ii) Three-dimensional (3D) phase-encoded EPI

An alternative approach to imaging the entire brain is to make use of the principle of phase encoding in the third dimension rather than acquiring data one slice at a time. This means that data are sampled from the entire 3D volume simultaneously but that many RF excitations of the system are necessary to build up a complete 3D set of k -space data, which is then processed using a 3D Fourier transform. An image matrix with N points in the third dimension can be acquired in the same time needed to image N slices in multislice EPI. In principle the technique has advantages because higher SNR can be obtained. The T_1 contrast between grey and white matter can also easily be manipulated, which may be advantageous in image realignment. A comparison between this method and 2D multislice imaging (Porter *et al.* 1997) showed similar activation images. However, through the use of navigator echoes it should be possible to achieve an improvement in the significance of the fMRI data with the 3D method and reduce their dependence on motion (Ramsey *et al.* 1998). Additionally, if high enough resolution is used, it should be possible to reduce signal dropout using 3D EPI (Wang *et al.* 1999).

(iii) Spiral scanning EPI

In the spiral version of EPI, k -space is sampled in a spiral rather than on a rectilinear trajectory. This method makes less demands on the gradient hardware and is rather less sensitive to some artefacts, in particular there is no Nyquist ghost. Field inhomogeneity causes image blurring rather than geometric distortion. The technique can be applied in either two dimensions, in which case multislicing as in conventional EPI is used, or as a 3D spiral in k -space. A comparison of both of these methods with conventional multislice EPI for functional imaging has been performed (Yang *et al.* 1998b) and this suggests that the temporal stability of the fMRI time-series can be better with spiral EPI. One disadvantage of the spiral techniques is that the data points in k -space have to be

regridded, which slows down the image processing. Another version of EPI which has been evaluated is a 2D spiral with phase encoding in the third dimension, which improves the signal drop-out problem and gives higher contrast to noise in the functional images (Yang *et al.* 1996; Lai & Glover 1998). Segmented spiral techniques with navigator echoes have also been successfully used for fMRI (Glover & Lai 1998).

(iv) *Echo-volumar imaging*

A final method worthy of mention is echo-volumar imaging (EVI) (Mansfield *et al.* 1989; Harvey & Mansfield 1996), which acquires all the data required to generate a volume image of the brain in a time of approximately 100 ms. EVI is technically very demanding and the use of a dedicated head gradient coil is very advantageous. It is unlikely to ever result in image matrices much larger than $32 \times 32 \times 32$; however, it does have the capacity to image BOLD contrast in the entire brain simultaneously. An example of the potential of this technique performed at 3 T (Hykin *et al.* 1995) is shown in figure 6. The data illustrate how EVI can be used to measure brain activity and has the potential to simultaneously monitor the dynamics of functional change over large cortical volumes.

4. LIMITATIONS OF fMRI METHODS

As a technique for imaging human brain function, fMRI has already demonstrated several advantages over PET and in the coming years $H_2^{15}O$ activation studies with PET may become redundant. The improvements in spatial and temporal resolution and sensitivity with fMRI are important, but probably the most significant advantage of fMRI is the absence of ionizing radiation. There is no limit with fMRI on the number of scans that a subject can undergo. This allows repeated measurements to be made, facilitating longitudinal studies over time and allowing the assessment of the reproducibility of activation images (Noll *et al.* 1997; McGonigle *et al.* 1999). Although it is possible that fMRI may largely replace PET for activation studies there are a number of limitations in using fMRI and currently there are certain experiments which can be better performed with PET. In §3(a) one of the most important limitations was discussed, the effect of field inhomogeneity rendering small volumes of brain tissue invisible. For example in the inferior temporal lobe, geometric distortion and signal drop-out are so severe on T_2^* -weighted EPI images that some language studies which have been successful with PET are difficult to reproduce with fMRI. Other than this difficulty, which is inherent to the imaging itself, other potential limitations are (i) the somewhat confined environment in which subjects lie in an MRI scanner; (ii) the need to operate other equipment in a large static magnetic field; (iii) acoustic noise generated by the imaging experiments; (iv) subject movement and physiological artefacts; and (v) possible peripheral nerve stimulation by the imaging gradients.

The internal diameter of a typical MRI scanner is 60 cm and the bore is between 1.5 and 2 m long. The subject's head is placed in an RF coil with a diameter and length of 30 cm. Many fMRI studies involve the presentation of a visual stimulus and in some cases video

presentation is required. This is commonly achieved using a projection system placed outside the magnet room, directed onto a screen which the subject views via a mirror. If the RF coil has an aperture above the eyes this system is very successful. However, particularly at higher fields, it is difficult to produce such open designs and it is necessary to make use of some form of goggles, either using prisms or optical fibre technology. Other types of stimulation apparatus need to be built to operate in a magnetic field. The restricted access of the MRI scanner also makes the performance of motor tasks more difficult, especially so because it is imperative that the subject does not move their head in tandem with the task.

EPI generates a loud ringing noise of about 100 dB SPL at frequencies of 1–2 kHz due to the switching of large gradient coil currents (up to 500 A) in the static field. For the subjects' protection it is imperative that ear defenders or plugs are worn during an fMRI experiment. The sound generated by the scanner means that auditory stimulation experiments are more difficult than with PET. By piping sound through ear defenders which provide about 20 dB attenuation, subjects can hear stimuli over the scanner noise. The sound created by the scanner is constant throughout the duration of the experiment and so the resultant activation of auditory cortex is largely cancelled out when a comparison between experimental conditions is made, although there is some evidence of acoustic masking of activation by scanner noise (Shah *et al.* 1997; Bandettini *et al.* 1998). This problem can be overcome at a cost of reduced data acquisition rates, by acquiring images in each volume very rapidly and then leaving gaps in time between clustered volume acquisitions (Hall *et al.* 1999; Eden *et al.* 1999). The use of a head-only gradient coil can reduce the noise level considerably.

The problem of subject movement during scanning has bedevilled fMRI since its earliest days, leading to the suggestion that many apparent activation results were the result of motion artefact (Hajnal *et al.* 1995). Today it is accepted that this is generally not the case, although the problem of motion artefacts is an important one. Even after precautions are taken to minimize head movement through the use of head restraints, head movement of 1–2 mm during scanning is common. In uncooperative patients it may be very much worse. Post-processing realignment methods (Friston *et al.* 1995) correct for rigid body translations and rotations of the head. However, these methods cannot account for all of the effects of movement. Errors in the realignment occur due to the limited width of the interpolation kernels which are constrained by computing time (Ashburner *et al.* 1997). An additional problem is the effect of T_1 relaxation, which can cause intensity fluctuations if there is movement during the scanning of the brain volume (Friston *et al.* 1996). This effect manifests itself differently in different imaging techniques and 3D EPI methods may not have the sensitivity to very small movements which multislice methods have. Even after correction, low-frequency drifts in the voxel time-course in fMRI data sets are quite common, although these may be largely due to very subtle fluctuations in magnetic field homogeneity (Smith *et al.* 1998). The most severe problem of motion arises in experiments which involve a motor task. This is because although only very small movement of the head may

result from hand movements for example, this movement may be highly correlated with the experimental design. This can lead to entirely false activations because changes in image intensity are then highly correlated with the comparison specified in the analysis. These apparent activations are typically found at sharp image boundaries and in areas of field inhomogeneity. Speaking or swallowing during the experiment introduce particularly severe movement-related problems. Even if the experimental timing is such that the verbal response falls during an interval between the acquisition of images it is unlikely that the subject's jaw will return to the same place and because of the complexity of tissue, bone and air-filled cavities in this part of the head, artefacts due to magnetic field changes in inferior brain structures can be very severe (Birn *et al.* 1998). Whether the problem of speaking during an fMRI acquisition can be overcome remains to be seen.

Improvements in the speed of image acquisition using EPI will inevitably involve the use of larger switched magnetic field gradients, but these are ultimately limited in strength by the need to avoid stimulation of nerves in the subject's body (Schmitt *et al.* 1998). Such stimulation results from the voltage, and hence current, induced in tissue as a result of the rapidly changing magnetic fields. The allowable rate of change of field (dB/dt) is limited by statutory guidelines to levels that largely prevent stimulation of peripheral nerves and which are consequently much less than the higher threshold at which stimulation of cardiac muscle might occur. Current fMRI experiments using EPI operate below these statutory levels, although modern gradient system technology will allow switching rates above the threshold. For a given gradient strength the peak dB/dt values in the body are much lower when using a head gradient insert, rather than a whole-body gradient coil, and such coils therefore offer the best route to reduced image acquisition times.

5. FUTURE DIRECTIONS OF fMRI METHODS

Most fMRI experiments are currently carried out at field strengths of 1.5 T, although there are a significant number of systems operating at higher magnetic fields of between 3.0 and 4.0 T (approximately 20 to 30 worldwide). Future developments of fMRI techniques and their applications are likely to be concentrated on these high-field systems which offer the potential of increased BOLD contrast as well as greater sensitivity in all MR imaging and spectroscopy experiments. New techniques are also being developed to provide more direct measurements of brain activity than BOLD contrast. These include spin labelling methods (see § 5(b)) and the use of hyperpolarized xenon to measure perfusion (Albert *et al.* 1994). Using optical pumping it is possible to massively increase the polarization of xenon (and helium), which can subsequently be introduced as a blood tracer with potentially high sensitivity. *In vivo* NMR spectroscopy allows the measurement of the concentration of brain metabolites and this technique has been applied to the measurement of metabolic flux during functional activity (Shulman *et al.* 1993). It has further been suggested (Shulman & Rothman 1998; Rothman *et al.*, this issue) that the measurement of glutamate to glutamine neurotransmitter

cycling with ^{13}C NMR spectroscopy allows an interpretation of fMRI studies more closely related to neurobiological processes rather than purely in psychological terms. Measurement of diffusion anisotropy via MRI-based diffusion tensor imaging allows the measurement of nerve fibre tract orientation in the brain (Teo *et al.* 1997). This potentially could lead to the non-invasive mapping of connectivity between cortical areas and illuminate links between brain structure and function. Preliminary studies using diffusion tensor imaging in conjunction with fMRI have been performed in the visual system (Werring *et al.* 1998*b*). Furthermore, in a study of motor recovery, fMRI activation has been correlated with preserved diffusion anisotropy (Werring *et al.* 1998*a*) suggesting that cortical pathways have been spared within the vicinity of a traumatic focal lesion.

The future should also see further integration of fMRI with other modalities measuring brain activity. The acquisition of EEG data while a subject lies in an MRI scanner has already been demonstrated (Ives *et al.* 1993; Lemieux *et al.* 1997; Allen *et al.* 1998) and offers the prospect of combining the excellent spatial resolution of the fMRI technique with the millisecond temporal resolution of EEG. The fMRI activation associated with interictal epileptic spikes has already been measured. The sensitivity of the electrophysiological signal appears sufficient to combine fMRI with normal event-related brain potentials. Transcranial magnetic stimulation has also been combined with fMRI (Bohning *et al.* 1998; Josephs *et al.* 1998*b*). This will allow the direct determination of the haemodynamic response resulting from transcranial magnetic stimulation-evoked neuronal activity and for transient dysfunction to be introduced during the course of an fMRI experiment.

In current fMRI studies the processing of the data is performed after completion of the scan on a computer remote from the MR imaging system. Typically it may take several hours to perform full data processing including image realignment. However, with the most up to date computer technology it is possible to perform online fMRI data processing if some of the stages of processing, such as image realignment, are removed (Cox & Jesmanowicz 1998). This opens up the opportunity to perform fMRI experiments in real time, which may have applications in presurgical planning for example, where the neurologist could monitor a patient's responses and adapt the stimulus presentation while the subject remains in the scanner.

(a) *The use of high field strength (> 3 T) for fMRI*

Higher field strength in MRI offers greater intrinsic SNR, which increases approximately linearly with field strength, and in many circumstances this increase can be translated into better spatial or temporal resolution in imaging and greater sensitivity in spectroscopy (see Gadian 1995). The best field strength for implementing fMRI experiments has been the subject of some debate. The ratio of BOLD signal change to noise that can be generated in an fMRI experiment depends upon the fractional change in the T_2^* relaxation rate ($\Delta R_2^*/R_2^*$) occurring during activation, as well as the base image SNR, and is maximized when TE is approximately T_2^* . Simulations predict that ΔR_2^* should vary approximately

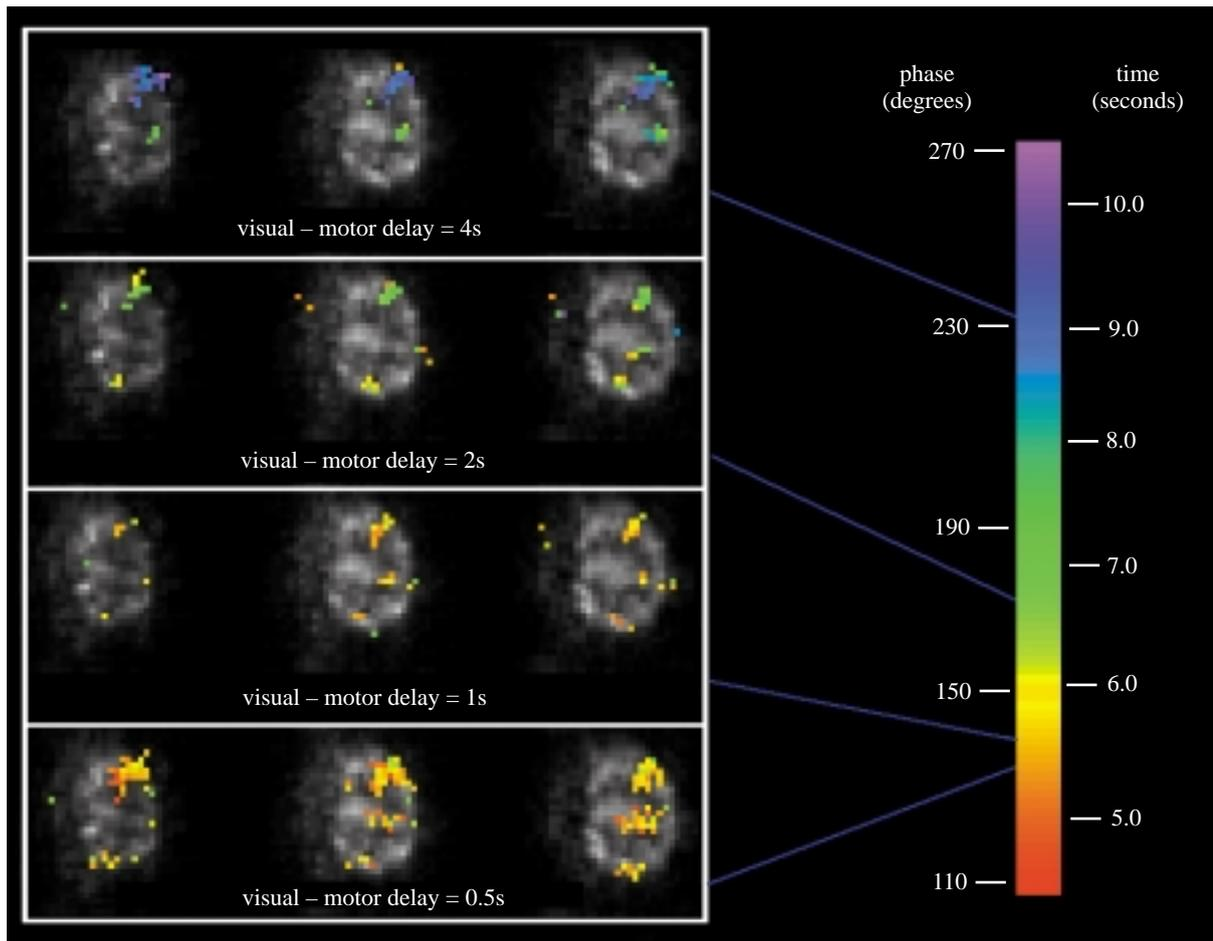


Figure 6. Echo-volumar images (EVIs) taken from a $32 \times 32 \times 16$ voxel data set acquired in a time of 116 ms at 3 T. Voxel size is $5 \text{ mm} \times 5 \text{ mm} \times 5 \text{ mm}$. The three axial slices displayed show activation in primary motor cortex (PMC) and supplementary motor areas (SMA). This study involved simultaneous measurement of activation in visual and motor cortex in a visually cued motor task, in which varying delays between the onset of visual stimulation and motor task execution (periodic button press) were employed. The coloured regions overlaid on the T_2^* -weighted EVI images, show the delay measured relative to the onset of the visual stimulus of the peak of activity in significantly activated motor areas. As expected this delay increases with the visual-motor delay. Simultaneous monitoring of activity in large cortical volumes allows direct comparison of the haemodynamic responses in different functional areas.

quadratically with field strength for small vessels and linearly for large vessels (Fisel *et al.* 1991; Ogawa *et al.* 1993), with experimental measurements in grey matter displaying a field dependence falling between these two extremes (Turner *et al.* 1993; Bandettini *et al.* 1994a). In measurements on visual cortex the ratio of ΔR_2^* to R_2^* has, however, been found experimentally to vary more slowly with field strength (Gati *et al.* 1997), but in conjunction with the linear increase in SNR this variation does lead to a hyperlinear increase in BOLD contrast-to-noise ratio with field strength, which makes high-field fMRI advantageous. The greater sensitivity to the capillary-based component compared with the effects of larger vessels (Gati *et al.* 1997) is an important benefit of working at high field. Uğurbil *et al.* (this issue) describe applications which are enabled by operation at high field.

It is not always possible, however, to achieve the predicted increase in contrast or to acquire data satisfactorily from the entire brain, because the increased large-scale susceptibility effects which occur at high magnetic field can prevent translation of the increased signal strength into improved image SNR and can limit

the usable echo time to sub-optimal values. The use of asymmetric or standard spin echo techniques, which at high field can give sufficient BOLD contrast with less or no signal drop-out offers a way around this problem. The specific problems relating to EPI at high field have seen considerable efforts already (Bowtell *et al.* 1994b; Kim *et al.* 1996; Hu & Le 1996; Yang *et al.* 1997a; Jesmanowicz *et al.* 1998) and particularly on the very high-field systems of 4.0 T and above, the optimization of EPI represents an important and very challenging hurdle if fMRI is to reap the potential benefits of the higher field. At high field a technique known as BURST imaging (Hennig & Hodapp 1993) may be useful in fMRI (Jakob *et al.* 1998) because BURST has the attractive feature of being a quiet imaging method and also is much less sensitive to image distortion than EPI. Its primary disadvantage is a relatively low SNR but at high field it may be advantageous for auditory studies.

In the light of the above, the recent successful production of human head images at the exceptionally high field of 8 T (Robitaille *et al.* 1998) is a very important development. While there are clearly a number of issues relating

to the penetration depth of higher frequency RF into the head and RF power deposition, as well as the increased susceptibility effects and the issue of the safety of exposure to very high static magnetic fields, it seems almost certain that the drive towards ever higher field strength for biological NMR will continue.

(b) *Measurement of tissue perfusion with MRI*

The direct measurement of cerebral perfusion has been addressed by a number of subtly different but related MRI techniques in recent years. These are referred to as arterial spin labelling (ASL) methods and involve the tagging of spins in a slab of tissue and measuring, in an imaging slice, their transfer from the circulation into brain tissue. The tagging of spins can be achieved by altering their magnetization state non-invasively, an advantage over other methods which use contrast agents. These ASL methods (e.g. EPSTAR (Edelman *et al.* 1994), FAIR (Kwong *et al.* 1994), QUIPS (Wong *et al.* 1996)) are all subtraction methods where the signal differences in the imaging slice are between tagged and untagged measurements. Measuring small differences on a large baseline signal is inherently subject to many sources of error. The signal changes produced by all of these methods depend upon the transit times of the tagged blood into the imaging slice and the T_1 relaxation rates of blood and brain water to generate a value for CBF. Therefore the accuracy of the CBF measurements and the specificity of the functional maps of CBF change may not be very high. However, these techniques show potential for making fMRI quantitative and it has been shown that similar functional maps can be achieved with perfusion methods as with BOLD (Yang *et al.* 1998a; Zhu *et al.* 1998), albeit with longer acquisition times and lower SNR. Considerable effort is currently being expended to refine further these methods and overcome the experimental and theoretical difficulties associated with them. It seems unlikely that ASL methods will become generally used for functional imaging studies because of their lower sensitivity but these techniques are already proving valuable in cross-validating the measurement of brain activity with PET and fMRI. In a recent study by Davis *et al.* (1998), perfusion-sensitive MRI and the breathing of carbon dioxide were used to calibrate BOLD contrast. This allows the measurement of changes in oxidative metabolism, and using a checkerboard stimulus it was found that oxygen consumption increased by 16% whereas blood flow increased by 45%, confirming the differential increase in rCBF and rCMRO₂ but demonstrating that oxidative metabolism is a significant component of functionally induced metabolic activity.

In concluding this review of the MRI methods which are being used in the measurement of human brain activity we hope that we have left the reader with a sense of the direction in which these techniques are heading. During its lifetime, MRI has never failed to amaze and delight its practitioners with the new applications and techniques which it holds in store. The use of MRI in functional neuroimaging has been one of its most spectacular successes and there are surely further surprises ahead about the ways in which we are able to

harness this quantum physics phenomenon to explore the workings of the human mind.

REFERENCES

- Albert, M. S., Cates, G. D., Driehuys, B., Happer, W., Saam, B., Springer, C. S. & Wishnia, A. 1994 Biological MRI using laser polarised ¹²⁹Xe. *Nature* **370**, 199–201.
- Allen, P. J., Polizzi, G., Krakow, K., Fish, D. R. & Lemieux, L. 1998 Identification of EEG events in the MR scanner: the problem of pulse artifact and a method for its subtraction. *NeuroImage* **8**, 229–239.
- Ashburner, J., Hutton, C., Grootenok, S., Turner, R. & Friston, K. 1997 Correction for movement related effects arising from data interpolation in fMRI time series. *NeuroImage* **5**, S453.
- Ashe, J. & Ugurbil, K. 1994 Functional imaging of the motor system. *Curr. Opin. Neurobiol.* **6**, 832–839.
- Bandettini, P. A. 1993 MRI studies of brain activation: dynamic characteristics. In *ISMRM workshop on functional MRI of the brain, Arlington, Virginia*, pp. 144–151.
- Bandettini, P. A., Wong, E. C., Hinks, R. S., Tikofsky, S. & Hyde, J. S. 1992 Time course EPI of human brain function during task activation. *Magn. Reson. Med.* **25**, 390–397.
- Bandettini, P. A., Wong, E. C., Jesmanowicz, A., Prost, R., Cox, R. W., Hinks, R. S. & Hyde, J. S. 1994a MRI of human brain activation at 0.5 T, 1.5 T and 3.0 T: comparisons of R₂' and functional contrast to noise ratio. In *Proceedings of the 2nd Meeting of ISMRM, San Francisco*, p. 434.
- Bandettini, P. A., Wong, E. C., Jesmanowicz, A., Hinks, R. S. & Hyde, J. S. 1994b Spin-echo and gradient-echo EPI of human brain activation using BOLD contrast: a comparative study at 1.5 T. *NMR Biomed.* **7**, 12–20.
- Bandettini, P. A., Kwong, K. K., Davis, T. L., Tootell, R. B. H., Wong, E. C., Fox, P. T., Belliveau, J. W., Weisskoff, R. M. & Rosen, B. R. 1997 Characterisation of cerebral blood oxygenation and flow changes during prolonged brain activation. *Hum. Brain Mapp.* **5**, 93–109.
- Bandettini, P. A., Jesmanowicz, A., Van Kylen, J., Birn, R. M. & Hyde, J. S. 1998 Functional MRI of brain activation induced by scanner acoustic noise. *Magn. Reson. Med.* **39**, 410–416.
- Belliveau, J. W., Kennedy, D. N., McKinstry, R. C., Buchbinder, B. R., Weisskoff, R. M., Cohen, M. S., Vevea, J. M., Brady, T. J. & Rosen, B. R. 1991 Functional mapping of the human visual cortex by magnetic resonance imaging. *Science* **254**, 716–719.
- Binder, J. R. 1997 Neuroanatomy of language processing studied with functional MRI. *Clin. Neurosci.* **4**, 87–94.
- Birn, R. M., Bandettini, P. A., Cox, R. W., Jesmanowicz, A. & Shaker, R. 1998 Magnetic field changes in the human brain due to swallowing or speaking. *Magn. Reson. Med.* **40**, 55–60.
- Bittar, R. G., Olivier, A., Sadikot, A., Andermann, F., Pike, G. B. & Reutens, D. C. 1998 Pre-surgical planning with fMRI: cross validation with PET. *NeuroImage* **7**, S64.
- Bohning, D. E., Shastri, A., Nahas, Z., Lorberbaum, J. P., Andersen, S. W., Dannels, W. R., Haxthausen, E. U., Vincent, D. J. & George, M. S. 1998 Echoplanar BOLD fMRI of brain activation induced by concurrent transcranial magnetic stimulation. *Invest. Radiol.* **33**, 336–340.
- Bowtell, R., McIntyre, D. J. O., Commandre, M. J., Glover, P. M. & Mansfield, P. 1994a Correction of geometric distortion in echo-planar images. In *Proceedings of the 2nd meeting of ISMRM, San Francisco*, p. 411.
- Bowtell, R., Mansfield, P., Coxon, R. J., Harvey, P. R. & Glover, P. M. 1994b High-resolution echo-planar imaging at 3.0 T. *MAGMA* **2**, 241–245.
- Boxerman, J. L., Bandettini, P. A., Kwong, K. K., Baker, J. R., Davis, T. L., Rosen, B. R. & Weisskoff, R. M. 1995 The intravascular contribution to fMRI signal change: Monte Carlo

- modeling and diffusion-weighted studies *in vivo*. *Magn. Reson. Med.* **34**, 4–10.
- Buxton, R. B. & Frank, L. R. 1997 A model for the coupling between cerebral blood flow and oxygen metabolism during neural stimulation. *J. Cerebr. Blood-Flow Metab.* **17**, 64–72.
- Buxton, R. B., Wong, E. C. & Frank, L. R. 1998 Dynamics of blood flow and oxygenation changes during brain activation: the balloon model. *Magn. Reson. Med.* **39**, 855–864.
- Chen, W., Zhu, X.-H., Kato, T., Andersen, P. & Ugurbil, K. 1998 Spatial and temporal differentiation of fMRI BOLD response in primary visual cortex of human brain during sustained visual stimulation. *Magn. Reson. Med.* **39**, 520–527.
- Clare, S., Hykin, J., Bowtell, R., Coxon, R. & Morris, P. G. 1996 Sub-millimetre resolution functional brain imaging with multislice interleaved EPI at 3.0 T. In *Proceedings of the 4th meeting of ISMRM, New York*, p. 1821.
- Cox, R. W. & Jesmanowicz, A. 1998 Whole brain real-time fMRI. In *Proceedings of the 6th meeting of ISMRM, Sydney*, p. 295.
- Davis, K. D., Taylor, S. J., Crawley, A. P., Wood, M. L. & Mikulis, D. J. 1997 Functional MRI of pain and attention related activations in the human cingulate cortex. *J. Neurophysiol.* **77**, 3370–3380.
- Davis, T. L., Kwong, K. K., Weisskoff, R. M. & Rosen, B. R. 1998 Calibrated functional MRI: mapping the dynamics of oxidative metabolism. *Proc. Natl Acad. Sci. USA* **95**, 1834–1839.
- DeYoe, E. A., Neitz, J., Bandettini, P. A., Wong, E. C. & Hyde, J. S. 1992 Time course of event related signal enhancement in visual and motor cortex. In *Proceedings of the 11th meeting of SMRM, Berlin*, p. 1824.
- Dymond, R. C. & Norris, D. G. 1997 Mechanism and echo time dependence of the fast response in fMR. *Magn. Reson. Med.* **38**, 1–6.
- Edelman, R. R., Siewert, B., Adamis, M., Gaa, J., Laub, G. & Wielopolski, P. 1994 Signal targeting with alternating radio frequency. *Magn. Reson. Med.* **31**, 233–238.
- Eden, G. F., Joseph, J. E., Brown, H. E., Brown, C. P. & Zeffiro, T. A. 1999 Utilising hemodynamic delay and dispersion to detect fMRI signal change without auditory interference: the behaviour interleaved gradients technique. *Magn. Reson. Med.* **41**, 13–20.
- Fisel, C. R., Ackerman, J. L., Buxton, R. B., Garrido, L., Belliveau, J. W., Rosen, B. R. & Brady, T. J. 1991 MR contrast due to microscopically heterogeneous magnet susceptibility: numerical simulations and applications to cerebral physiology. *Magn. Reson. Med.* **17**, 336–347.
- Fletcher, P. C., Frith, C. D. & Rugg, M. D. 1997 The functional neuroanatomy of episodic memory. *Trends Neurosci.* **20**, 213–218.
- Fox, P. T. & Raichle, M. E. 1986 Focal physiological uncoupling of cerebral blood flow and oxidative metabolism during somatosensory stimulation in human subjects. *Proc. Natl Acad. Sci. USA* **83**, 1140–1144.
- Fox, P. T., Raichle, M. E., Mintun, M. A. & Dence, C. 1988 Non-oxidative glucose consumption during focal physiologic neural activity. *Science* **241**, 462–464.
- Frackowiak, R. S. J., Friston, K. J., Frith, C. D., Dolan, R. J. & Mazziotta, J. C. (eds) 1997 *Human brain function*. Academic Press.
- Frahm, J., Merboldt, K.-D. & Hancicke, W. 1993 Functional MRI of human brain activation at high spatial resolution. *Magn. Reson. Med.* **29**, 139–144.
- Frahm, J., Merboldt, K.-D., Hancicke, W., Kleinschmidt, A. & Boecker, H. 1994 Brain or vein—oxygenation or flow? On signal physiology in functional MRI of human brain activation. *NMR Biomed.* **7**, 45–53.
- Frahm, J., Kruger, G., Merboldt, K.-D. & Kleinschmidt, A. 1996 Dynamic uncoupling and recoupling of perfusion and oxidative metabolism during focal brain activation in man. *Magn. Reson. Med.* **35**, 143–148.
- Fransson, P., Kruger, G., Merboldt, K.-D. & Frahm, J. 1998 Temporal characteristics of oxygenation-sensitive MRI responses to visual activation in humans. *Magn. Reson. Med.* **39**, 912–919.
- Friston, K. J., Jezzard, P. & Turner, R. 1994 Analysis of functional MRI time-series. *Hum. Brain Mapp.* **1**, 153–171.
- Friston, K. J., Ashburner, J., Frith, C. D., Poline, J.-B., Heather, J. D. & Frackowiak, R. S. J. 1995 Spatial registration and normalization of images. *Hum. Brain Mapp.* **2**, 165–189.
- Friston, K. J., Williams, S., Howard, R., Frackowiak, R. S. J. & Turner, R. 1996 Movement-related effects in fMRI time-series. *Magn. Reson. Med.* **35**, 346–355.
- Friston, K. J., Josephs, O., Rees, G. & Turner, R. 1998a Nonlinear event-related responses in fMRI. *Magn. Reson. Med.* **39**, 41–52.
- Friston, K. J., Fletcher, P., Josephs, O., Rugg, M. D. & Turner, R. 1998b Event-related fMRI: characterising differential responses. *NeuroImage* **7**, 30–40.
- Gadian, D. G. 1995 *NMR and its applications to living systems*, 2nd edn. Oxford University Press.
- Gati, J. S., Menon, R. S., Ugurbil, K. & Rutt, B. K. 1997 Experimental determination of the BOLD field strength dependence in vessels and tissue. *Magn. Reson. Med.* **38**, 296–302.
- Glover, G. H. & Lai, S. 1998 Self-navigated spiral fMRI: interleaved versus single shot. *Magn. Reson. Med.* **39**, 361–368.
- Graveline, C., Mikulis, D., Crawley, A. & Hwang, P. A. 1998 Regionalisation evidence of sensorimotor plasticity pre and post hemispherectomy in children with epilepsy. FMRI and clinical studies. *NeuroImage* **7**, S483.
- Grootoink, S., Howseman, A. M., Blakemore, S.-J., Hutton, C., Ashburner, J. & Turner, R. 1998 Assessment of motion artefacts in fMRI time series affected by task correlated subject motion. *NeuroImage* **7**, S600.
- Haacke, E. M. (and 12 others) 1994 2D and 3D high resolution gradient echo functional imaging of the brain: venous contributions to signal in motor cortex studies. *NMR Biomed.* **7**, 54–62.
- Haase, A., Frahm, J., Matthaei, D., Hancicke, W. & Merboldt, K.-D. 1986 FLASH imaging. Rapid NMR imaging using low flip-angle pulses. *J. Magn. Reson.* **67**, 258–266.
- Hajnal, J. V., Bydder, G. M. & Young, I. R. 1995 fMRI: does correlation imply activation? *NMR Biomed.* **8**, 97–100.
- Hall, D. A., Haggard, M. P., Akeroyd, M. A., Palmer, A. R., Summerfield, A. P., Elliott, M. R., Gurney, E. M. & Bowtell, R. W. 1999 ‘Sparse’ temporal sampling in auditory fMRI. *Hum. Brain Mapp.* (In the press.)
- Harvey, P. & Mansfield, P. 1996 Echo-volumar imaging (EVI) at 0.5 T: first whole-body volunteer studies. *Magn. Reson. Med.* **35**, 80–88.
- Hennig, J. & Hodapp, M. 1993 BURST imaging. *MAGMA* **1**, 39–48.
- Howseman, A. M., Porter, D. A., Hutton, C., Josephs, O. & Turner, R. 1998 Blood oxygenation level dependent signal time courses during prolonged visual stimulation. *Magn. Reson. Imaging* **16**, 1–11.
- Howseman, A. M., Grootoink, S. G., Porter, D. A., Ramdeen, J., Holmes, A. P. & Turner, R. 1999 The effect of slice order and thickness on fMRI activation data using multislice echo-planar imaging. *NeuroImage* **9**, 363–376.
- Hu, X. & Le, T. H. 1996 Artifact reduction in EPI with phase-encoded reference scan. *Magn. Reson. Med.* **36**, 166–171.
- Hu, X., Le, T. H. & Ugurbil, K. 1997 Evaluation of the early response in fMRI in individual subjects using short stimulus duration. *Magn. Reson. Med.* **37**, 877–884.
- Hykin, J., Coxon, R., Bowtell, R. W., Glover, P. & Mansfield, P. 1995 Temporal differences in functional activation between

- separate regions of the brain investigated with single shot EVI. In *Proceedings of the 3rd meeting of ISMRM, Nice*, p. 451.
- Ives, J. R., Warach, S., Schmitt, F., Edelman, R. R. & Schomer, D. L. 1993 Monitoring the patient's EEG during echo-planar MRI. *Electroencephalogr. Clin. Neurophysiol.* **87**, 417–420.
- Jackson, G. D., Connelly, A., Cross, J. H., Gordon, I. & Gadian, D. G. 1994 Functional magnetic resonance imaging of focal seizures. *Neurology* **44**, 850–856.
- Jakob, P. M., Schlaug, G., Griswold, M., Lovblad, K. O., Thomas, R., Ives, J. R., Matheson, J. K. & Edelman, R. R. 1998 Functional BURST imaging. *Magn. Reson. Med.* **40**, 614–621.
- Janz, C., Speck, O. & Hennig, J. 1997 Time resolved measurements of brain activation after a short visual stimulus: new results on the physiological mechanisms of the cortical response. *NMR Biomed.* **10**, 222–229.
- Jesmanowicz, A., Bandettini, P. A. & Hyde, J. S. 1998 Single-shot half k-space high-resolution gradient-recalled EPI for fMRI at 3 tesla. *Magn. Reson. Med.* **40**, 754–762.
- Jezzard, P. & Balaban, R. S. 1995 Correction for geometric distortion in echo-planar images from B_0 field variations. *Magn. Reson. Med.* **34**, 65–73.
- Josephs, O., Turner, R. & Friston, K. 1998a Event-related fMRI. *Hum. Brain Mapp.* **6**, 243–248.
- Josephs, O., Athwal, B. S., Mackinnon, C., Rothwell, J. & Turner, R. 1998b Transcranial magnetic stimulation with simultaneous undistorted functional magnetic resonance imaging. In *Proceedings of the 4th meeting of the British chapter of ISMRM, Nottingham*, p. 12.
- Jueptner, M. & Weiller, C. 1995 Does measurement of regional cerebral blood flow reflect synaptic activity? Implications for PET and fMRI. *NeuroImage* **2**, 148–156.
- Kim, S.-G., Hendrich, K., Hu, X., Merkle, H. & Ugurbil, K. 1994 Potential pitfalls of functional MRI using conventional gradient-recalled echo techniques. *NMR Biomed.* **7**, 69–74.
- Kim, S.-G., Hu, X., Adriany, G. & Ugurbil, K. 1996 Fast interleaved echo-planar imaging with navigator: high resolution anatomic and functional images at 4 tesla. *Magn. Reson. Med.* **35**, 895–902.
- Kim, S.-G., Richter, W. & Ugurbil, K. 1997 Limitations of temporal resolution in functional fMRI. *Magn. Reson. Med.* **37**, 631–636.
- Kruger, G., Kleinschmidt, A. & Frahm, J. 1996 Dynamic MRI sensitised to cerebral blood oxygenation and flow during sustained activation of human visual cortex. *Magn. Reson. Med.* **35**, 797–800.
- Kwong, K. K. (and 12 others) 1992 Dynamic magnetic resonance imaging of human brain activity during primary sensory stimulation. *Proc. Natl Acad. Sci. USA* **89**, 5675–5679.
- Kwong, K. K., Chesler, D. A., Weisskoff, R. M. & Rosen, B. 1994 Perfusion MR imaging. In *Proceedings of the 2nd meeting of ISMRM, San Francisco*, p. 1005.
- Lai, S. & Glover, G. H. 1998 Three dimensional spiral fMRI technique: a comparison with 2D spiral acquisition. *Magn. Reson. Med.* **39**, 68–78.
- Lai, S., Hopkins, A., Haacke, E., Li, D., Wasserman, B., Buckley, P., Friedman, L., Meltzer, H., Hedera, P. & Friedland, R. 1993 Identification of vascular structures as a major source of signal contrast in high resolution 2D and 3D functional activation imaging of the motor cortex at 1.5 T: preliminary results. *Magn. Reson. Med.* **30**, 387–392.
- Lassen, N. A., Ingvar, D. H., Raichle, M. E. & Friberg, L. (eds) 1991 *Brain work and mental activity. Quantitative studies with radioactive tracers*. Copenhagen: Munksgaard.
- Lee, A. T., Glover, G. H. & Meyer, C. H. 1995 Discrimination of large venous vessels in time-course spiral blood-oxygen-level-dependent magnetic resonance functional neuroimaging. *Magn. Reson. Med.* **33**, 745–754.
- Lehericy, S., Duffau, H., Cornu, P., Capelle, L., Sichez, J.-P., Fohanno, D., Philippon, J., Le Bihan, D. & Marsault, C. 1998 Presurgical fMRI mapping of cortical motor areas in patients with brain tumours: comparison with intrasurgical stimulation. *NeuroImage* **7**, S475.
- Leifer, D., Lacadie, C., Fulbright, R. K., Zhong, J., Graham, G. D. & Gore, J. C. 1998 Functional MRI studies of motor recovery after stroke. *NeuroImage* **7**, S475.
- Lemieux, L., Allen, P. J., Franconi, F., Symms, M. R. & Fish, D. R. 1997 Recording of EEG during fMRI experiments: patient safety. *Magn. Reson. Med.* **38**, 943–952.
- Lotze, M., Grodd, W., Erb, M., Larbig, W., Flor, H. & Birbaumer, 1998 fMRI of cortical reorganisation in the primary motor and sensory cortex after traumatic upper limb amputation. *NeuroImage* **7**, S17.
- McCarthy, G. 1998 Preoperative evaluation of neurosurgical patients with fMRI. In *Proceedings of the 6th meeting of ISMRM, Sydney*, p. 292.
- McGonigle, D. J., Howseman, A. M., Athwal, B. S., Friston, K. J., Frackowiak, R. S. J. & Holmes, A. P. 1999 An examination of inter-session differences in fMRI. In *Proceedings of the 5th international conference on functional mapping of the human brain, Dusseldorf*. (Submitted.)
- Malonek, D. & Grinvald, A. 1996 Interactions between electrical activity and cortical microcirculation revealed by imaging spectroscopy: implications for functional brain imaging. *Science* **272**, 551–554.
- Mansfield, P. 1977 Multi-planar image formation using NMR spin echoes. *J. Phys. C* **10**, L55–L58.
- Mansfield, P., Howseman, A. M. & Ordidge, R. J. 1989 Volumar imaging using NMR spin echoes: echo-volumar imaging (EVI) at 0.1 T. *J. Phys. E: Sci. Instrum.* **22**, 324–330.
- Menon, R. S., Ogawa, S., Tank, D. W. & Ugurbil, K. 1993 4 tesla gradient recalled echo characteristics of photic stimulation-induced signal changes in the human primary visual cortex. *Magn. Reson. Med.* **30**, 380–386.
- Menon, R. S., Ogawa, S., Hu, X., Strupp, J. P., Anderson, P. & Ugurbil, K. 1995 BOLD based functional MRI at 4 tesla includes a capillary bed contribution: echo-planar imaging correlates with previous optical imaging using intrinsic signals. *Magn. Reson. Med.* **33**, 453–459.
- Noll, D. C., Genovese, C. R., Nystrom, L. E., Vazquez, A. L., Forman, S. D., Eddy, W. F. & Cohen, J. D. 1997 Estimating test-retest reliability in functional MR imaging. II. Application to motor and cognitive activation studies. *Magn. Reson. Med.* **38**, 508–517.
- Ogawa, S., Lee, T. M., Kay, A. R. & Tank, D. W. 1990 Brain magnetic resonance imaging with contrast dependent on blood oxygenation. *Proc. Natl Acad. Sci. USA* **87**, 9868–9872.
- Ogawa, S., Tank, D. W., Menon, R., Ellerman, J. G., Kim, S. G., Merkle, K. & Ugurbil, K. 1992 Intrinsic signal changes accompanying sensory stimulation: functional brain mapping with magnetic resonance imaging. *Proc. Natl Acad. Sci. USA* **89**, 5951–5955.
- Ogawa, S., Menon, R. S., Tank, D. W., Kim, S.-G., Merkle, H., Ellermann, J. M. & Ugurbil, K. 1993 Functional brain mapping by blood oxygenation level dependent contrast magnetic resonance imaging. A comparison of signal characteristics with a biophysical model. *Biophys. J.* **64**, 803–812.
- Phillips, M. L. (and 11 others) 1997 A specific neural substrate for perceiving facial expressions of disgust. *Nature* **389**, 495–498.
- Porter, D. A., Howseman, A. M., Josephs, O. & Turner, R. 1997 A comparison of 2D and 3D EPI for whole brain fMRI. In *Proceedings of the 5th meeting of ISMRM, Vancouver*, p. 1621.
- Price, C. J., Veltman, D. J., Ashburner, J., Josephs, O. & Friston, K. J. 1999 The critical relationship between the timing of stimulus presentation and data acquisition in blocked designs with fMRI. *NeuroImage*. (In the press.)

- Ramsey, N. F., Van den Brink, J. S., Van Muiswinkel, A. M. C., Folkers, P. J. M., Moonen, C. T. W., Jansma, J. M. & Kahn, R. S. 1998 Phase navigator correction in 3D fMRI improves detection of brain activation: quantitative assessment with a graded motor activation procedure. *NeuroImage* **8**, 240–248.
- Reber, P. J., Wong, E. C., Buxton, R. B. & Frank, L. R. 1998 Correction of off resonance-related distortion in echo-planar imaging using EPI-based field maps. *Magn. Reson. Med.* **39**, 328–330.
- Rees, G. E., Howseman, A. M., Josephs, O., Frith, C. D., Friston, K. J., Frackowiak, R. S. J. & Turner, R. 1997 Characterising the relationship between BOLD contrast and regional cerebral blood flow measurements by varying the stimulus presentation rate. *NeuroImage* **6**, 270–278.
- Robitaille, P. M. (and 13 others) 1998 Human magnetic resonance imaging at 8 T. *NMR Biomed.* **11**, 263–265.
- Rosen, B. R., Buckner, R. L. & Dale, A. M. 1998 Event-related functional MRI: past, present, and future. *Proc. Natl Acad. Sci. USA* **95**, 773–780.
- Savoy, R. L., Bandettini, P. A., O'Craven, K. M., Kwong, K. K., Davis, T. L., Baker, J. R., Weisskoff, R. M. & Rosen, B. R. 1995 Pushing the temporal resolution of fMRI: studies of very brief stimuli, onset variability and asynchrony, and stimulus-correlated changes in noise. In *Proceedings of the 3rd meeting of ISMRM, Nice*, p. 450.
- Schmitt, F., Stehling, M. K. & Turner, R. (eds) 1998 *Echo-planar imaging*. Berlin: Springer.
- Schneider, F., Grodd, W., Weiss, U., Klose, U., Mayer, K. R., Nagele, T. & Gur, R. C. 1997 Functional MRI reveals left amygdala activation during emotion. *Psychiat. Res.* **76**, 75–82.
- Shah, N. J., Jancke, L., Gross-Ruyken, M. L., Posse, S. & Muller-Gartner, H. W. 1997 How does acoustic masking noise affect the auditory cortex during phonetic discrimination? *NeuroImage* **5**, S195.
- Shulman, R. G. & Rothman, D. L. 1998 Interpreting functional studies in terms of neurotransmitter cycling. *Proc. Natl Acad. Sci. USA* **95**, 11993–11998.
- Shulman, R. G., Blamire, A. M., Rothman, D. L. & McCarthy, G. 1993 Nuclear magnetic resonance imaging and spectroscopy of human brain function. *Proc. Natl Acad. Sci. USA* **90**, 3127–3133.
- Smith, A. M., Lewis, B. K., Ruttimann, U. E., Ye, F. Q., Sinnwell, T. M., Yang, Y., Duyn, J. H. & Frank, J. A. 1998 Investigation of low frequency drift in fMRI signal. In *Proceedings of the 15th meeting of ESMRMB, Geneva*, p. 182.
- Song, A. W., Wong, E. W., Tan, S. G. & Hyde, J. S. 1996 Diffusion weighted fMRI at 1.5 T. *Magn. Reson. Med.* **35**, 155–158.
- Stables, L. A., Kennan, R. P. & Gore, J. C. 1998 Asymmetric spin-echo of magnetically inhomogeneous system: theory, experiment and numerical studies. *Magn. Reson. Med.* **40**, 432–442.
- Teo, P. C., Sapiro, G. & Wandell, B. A. 1997 Creating connected representations of cortical grey matter for functional MRI visualisation. *IEEE Trans. Med. Imag.* **16**, 852–863.
- Thulborn, K. R., Chang, S. Y., Shen, G. X. & Voyvodic, J. T. 1997 High resolution echo-planar fMRI of human visual cortex at 3.0 tesla. *NMR Biomed.* **10**, 183–190.
- Thulborn, K. R., Martin, C., Davis, D., Erb, P., Carpenter, P. & Just, M. 1998 Recovered cognitive function following stroke assessed by fMRI using a language comprehension paradigm. In *Proceedings of the 6th meeting of ISMRM, Sydney*, p. 107.
- Tootell, R. B. H., Hadjikhani, N. K., Mendola, J. D., Marrett, S. & Dale, A. M. 1998 From retinotopy to recognition: fMRI in human visual cortex. *Trends Cogn. Sci.* **2**, 174–183.
- Turner, R., Le Bihan, D., Moonen, C. T. W., Despres, D. & Frank, J. 1991 Echo-planar time course MRI of cat brain oxygenation changes. *Magn. Reson. Med.* **22**, 159–166.
- Turner, R., Jezzard, P., Wen, H., Kwong, K. K., Le Bihan, D., Zeffiro, T. & Balaban, R. S. 1993 Functional mapping of the human visual cortex at 4 and 1.5 tesla using deoxygenation contrast EPI. *Magn. Reson. Med.* **29**, 277–279.
- Wang, J. J., Howseman, A. M., Josephs, O., Porter, D., Turner, R. & Ordidge, R. J. 1999 Signal dropout in 3D echo-planar imaging. In *Proceedings of the 4th meeting of the British chapter of ISMRM, Nottingham*, p. 22.
- Weisskoff, R. M., Zuo, C. S., Boxerman, J. L. & Rosen, B. R. 1994 Microscopic susceptibility variation and transverse relaxation: theory and experiment. *Magn. Reson. Med.* **31**, 601–610.
- Werring, D. J. (and 10 others) 1998a Motor recovery visualised by functional MRI and diffusion tensor imaging. *NeuroImage* **7**, S477.
- Werring, D. J., Clark, C. A., Parker, G. J. M., Barker, G. J., Symms, M., Franconi, F., Miller, D. H. & Thompson, A. J. 1998b Investigating the relationship between brain structure and function: combining diffusion tensor imaging with functional MRI in the visual system. *NeuroImage* **7**, S34.
- Wong, E. C., Buxton, R. B. & Frank, L. R. 1996 Quantitative imaging of perfusion using a single subtraction (QUIPSS). *NeuroImage* **3**, S5.
- Yang, Q. X., Dardzinski, B. J., Li, S., Eslinger, P. J. & Smith, M. B. 1997a Multi-gradient echo with susceptibility inhomogeneity compensation (MGESIC): demonstration of fMRI in the olfactory cortex at 3.0 T. *Magn. Reson. Med.* **37**, 331–335.
- Yang, X., Hyder, F. & Shulman, R. G. 1997b Functional MRI BOLD signal coincides with electrical activity in the rat whisker barrels. *Magn. Reson. Med.* **38**, 874–877.
- Yang, Y. (and 10 others) 1996 Fast 3D functional magnetic resonance imaging at 1.5 T with spiral acquisition. *Magn. Reson. Med.* **36**, 620–626.
- Yang, Y., Frank, J. A., Hou, L., Ye, F. Q., McLaughlin, A. C., Duyn, J. H. 1998a Multislice imaging of quantitative cerebral perfusion with pulsed arterial spin labelling. *Magn. Reson. Med.* **39**, 825–832.
- Yang, Y., Glover, G. H., Van Gelderen, P., Patel, A. C., Mattay, V. S., Frank, J. A. & Duyn, J. H. 1998b A comparison of fast MR scan techniques for cerebral activation studies at 1.5 tesla. *Magn. Reson. Med.* **39**, 61–67.
- Zhong, J., Kennan, R. P., Fulbright, R. K. & Gore, J. C. 1998 Quantification of intravascular and extravascular contributions to BOLD effects induced by alteration in oxygenation or intravascular contrast agents. *Magn. Reson. Med.* **40**, 526–536.
- Zhu, X.-H., Kim, S.-G., Andersen, P., Ogawa, S., Ugurbil, K. & Chen, W. 1998 Simultaneous oxygenation and perfusion imaging study of functional activity in primary visual cortex at different visual stimulation frequency: quantitative correlation between BOLD and CBF changes. *Magn. Reson. Med.* **40**, 703–711.